

The parametric resonance — from LEGO Mindstorms to cold atoms

Tomasz Kawalec and Aleksandra Sierant

Marian Smoluchowski Institute of Physics, Jagiellonian University, ul. Łojasiewicza 11, 30-348 Krakow, Poland

E-mail: tomasz.kawalec@uj.edu.pl

Abstract. We show an experimental setup based on a popular LEGO Mindstorms set, allowing to both observe and investigate the parametric resonance phenomenon. The presented method is simple but covers a variety of student activities like embedded software development, conducting measurements, data collection and analysis. It may be used during science shows, as part of the student projects and to illustrate the parametric resonance in mechanics or even quantum physics, during lectures or classes. The parametrically driven LEGO pendulum gains energy in a spectacular way, increasing its amplitude from 10° to about 100° within a few tens of seconds. We provide also a short description of a wireless absolute orientation sensor that may be used in quantitative analysis of driven or free pendulum movement.

PACS numbers: 01.50.My, 01.50.Wg, 45.40.-f

Submitted to: *Eur. J. Phys.*

1. Introduction

The parametric resonance is a well known phenomenon which can frequently be observed in many fields of physics and engineering. M. Faraday was likely the first one to recognize this effect — with surface waves on a liquid [1]. The parametric resonance appears in mechanics from micromechanical systems, through playground swings and architecture to ships sailing an ocean [2, 3].

This kind of resonance appears as a result of periodic changes of one of the oscillator parameters, in contrast to a common case of forced oscillations. In the case of a simple pendulum it may be its length modulation or an effective modulation of the gravitational acceleration g . The latter case is realized by forcing oscillations of the point of suspension. The analysis of the parametric excitation shows that the frequency of the modulation should be twice the natural frequency ω_0 of the system or be a subharmonic of $2\omega_0$. In the model system, the energy gain of the oscillator is proportional to its energy. Thus, the energy increases exponentially in time and the amplitude increase is unlimited, also in the presence of friction — see e.g. [4].

Originally, the idea of the presentation of the parametric resonance with LEGO Mindstorms bricks appeared during preparation of lectures on experimental techniques in contemporary atomic physics for graduate students [5]. There are few simple experiments that could be used to increase the attractiveness of such a lecture at this level. For example, the two laser interference described in our previous article (see Ref. [6]), although quite spectacular, is relatively complicated. On the other hand the LEGO Mindstorms sets have been used so far both in research and didactics (see e.g. Refs. [7, 8]). They are also routinely used as a main tool in student projects in engineering and mechatronics. We note that *LEGO* and *Mindstorms* are trademarks of the LEGO Group.

The parametric resonance phenomenon has been extensively explored in the literature, both in articles and books, from the point of view of classical and quantum physics (see e.g. [4, 9]). The didactic articles provide elementary as well as calculus based descriptions [10, 11, 12, 13]. Several articles have been devoted to the quantitative analysis of pumping a swing and what is the contribution of the parametric resonance to this process [14, 15, 16, 17, 18]. On the other hand, there seem to be only a few descriptions of the feasible experimental demonstrations. Some information is given in Refs. [11, 17, 14, 19, 20] and three experiments are described in details in Ref. [21]. Thus, in this article we present only a short mathematical approach and focus mainly on the practical realizations of the parametric resonance demonstration.

2. Basic mathematical description

The model system for the parametrically driven pendulum is depicted in Fig. 1 (a). A simple pendulum of the length l_0 is characterized by a natural frequency ω_0 . The l_0 length plays a role of a reduced length of our real pendulum described later. The length

(one of the exemplary pendulum parameters) is modulated with a frequency ω , being close to the doubled natural frequency ω_0 . The Lagrangian L of the system is:

$$L = \frac{1}{2}ml(t)^2\dot{\varphi}^2 + \frac{1}{2}m\dot{l}(t)^2 - (-mgl(t)\cos\varphi), \text{ where} \quad (1)$$

$$l(t) = l_0(1 + f(t)). \quad (2)$$

We use standard notation: m is mass of the pendulum, $l(t)$ is its reduced length, g is gravitational acceleration and φ is angle of inclination from vertical. The function $f(t)$ describes the pendulum length modulation. In the simplest case $f(t) = \cos(\omega t)$ with ω being constant and close to $2\omega_0$. However, such a modulation turns out to be inefficient in the case of a pendulum due to a period-amplitude dependency. Indeed, the increasing amplitude is accompanied by a decrease in the natural frequency ω_0 and removes the system from the parametric resonance condition. This problem is avoided in a straightforward way on a swing. A child pumps the swing in a kind of a closed loop system — observing the phase of a swing and adjusting accordingly his/her movement (squatting, straightening, leaning). Thus, in the case of our open loop configuration, the modulation frequency has to be adjusted in a different way, as will be discussed in Sec. 3.1.

To find the evolution of the angle φ we solve the Euler-Lagrange equation, following Ref. [14]. However, we first complement the equation with the dissipative term $\partial P/\partial\dot{\varphi}$ [22]:

$$\frac{d}{dt}\frac{\partial L}{\partial\dot{\varphi}} - \frac{\partial L}{\partial\varphi} + \frac{\partial P}{\partial\dot{\varphi}} = 0, \text{ where} \quad (3)$$

$$\frac{\partial P}{\partial\dot{\varphi}} = -F_\varphi = \alpha l^2\dot{\varphi}. \quad (4)$$

P is so called power or dissipation function, F_φ is a generalized force for the generalized coordinate φ and α is a damping constant (we have checked that a viscous friction dominates in our case). Finally, putting together Eqs. 1-4 we get:

$$\left(1 + \frac{f(t)}{l_0}\right)\ddot{\varphi} = -\frac{g}{l_0}\sin\varphi - 2\frac{\dot{f}(t)}{l_0}\dot{\varphi} - \frac{\alpha}{m}\dot{\varphi}\left(1 + \frac{f(t)}{l_0}\right). \quad (5)$$

Since the amplitude of the oscillations is large, the small angle approximation cannot be used. If we take $f(t) = 0$ in Eq. 5, we get the common equation for a damped pendulum. The value of α/m may be easily found experimentally by analysis of damped oscillations for the unmodulated pendulum. The $f(t)$ function may be either modelled or (as in our case) found on the basis of the automatic measurement of the modulating motor phase. The above approach is not strictly rigorous since, as we shall see in Sec. 3.1, the f function depends to some extent also on φ and $\dot{\varphi}$. However, an inclusion of this effect is difficult and presumably not advantageous from the didactic point of view.

3. Description of the experimental setup

The pendulum with a modulated length was constructed out of standard LEGO bricks included in the 8547 LEGO Mindstorms NXT set. A similar pendulum may be created on the basis of an educational version (set number 9797) or a newer set called EV3. These sets, and especially the educational one, are very popular at the technical and engineering as well as physics and computer science faculties. A general picture and a detailed view of the main part are shown in Fig. 1 (b). The real length of the pendulum is 54.5 cm and the measured reduced length is 40.4 cm. The upper motor is powered and controlled by a dedicated controller (often called an “intelligent brick”) and its axle rotates with a speed set by the user. The rotational motion is converted to a vertical motion of the lower part of the pendulum, as shown in magnification in the figure. The pendulum is loaded either with an additional unconnected motor or (optionally) with a wireless sensor described in Sec. 3.3. The controller is programmed from a computer, using a dedicated LEGO Mindstorms software. The program for the pendulum is very simple and allows the user to change the power of the motor with two switches with the resolution of 1%. Additionally, depending on the needs, other features were added, like measurement and data logging of the motor phase or pendulum inclination in real time, as described in the next two subsections. The period of the motor axle revolution has to be precisely two times smaller than the period of the pendulum (being in our case about 1.3 s). According to our experience, for the given conditions, there is only one or at most two values of the motor power (expressed in percents) when the effective parametric excitation may be achieved. Typically, the power of the motor was in the range of 65-80%, depending on the type of the batteries used and their condition. We have measured that the change of the power by 1% changes the duration of one motor revolution by 8-10 ms.

3.1. Basic setup

It is well known that in the general case the period of the pendulum depends on the amplitude of its oscillations. For example, the period calculated from the complete elliptic integral of the first kind for the amplitudes of 70° , 90° and 110° is by 10%, 18% and 30% greater than the one for the small amplitude. Thus, to achieve the efficient parametric excitation of the pendulum, the period of the modulating motor should be properly tuned. To avoid complicated solutions we have tested the simplest approach. We let the motor power be controlled in the open loop instead of the closed one. This way the controller does not try to keep the user-defined speed of the motor at a constant level when it experiences resistance or slippage. In the case of our pendulum, for increasing amplitude, the increasing centripetal force acting on the bob increases also the load of the motor, slowing down mainly the contraction phase of the pendulum. Thus the system adjusts the modulation period to the increasing period of the pendulum. In Fig. 2 (a) and (b) we show two exemplary pictures illustrating the parametric resonance — taken at the initial and maximum inclination. On the basis of the motor angle recorded

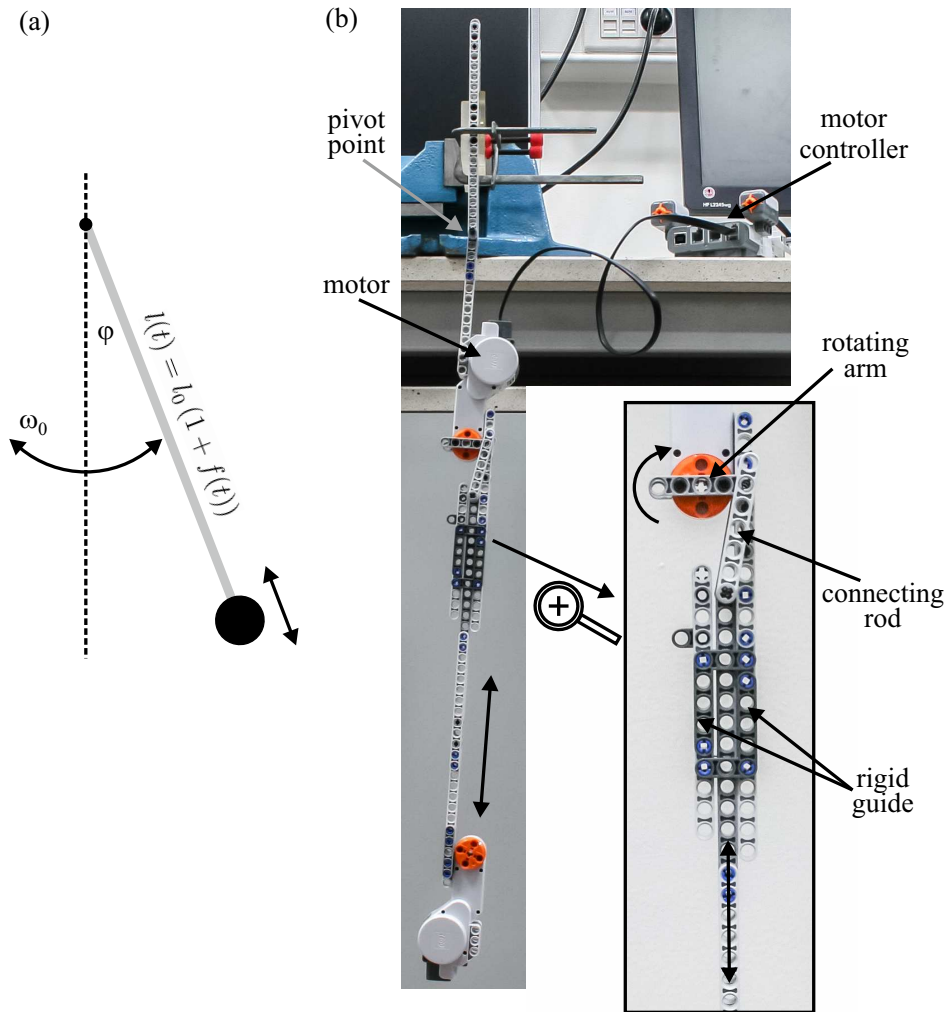


Figure 1. Pendulum with a modulated length: (a) simple model — the pendulum characterized by a natural frequency ω_0 and a reduced length l_0 , modulated quasiperiodically, as described by $l(t)$. The $f(t)$ function has a cosine-like form in our case (see text). The angle of inclination is φ , (b) basic setup: the rotational motion of the upper motor axle is converted to a vertical motion of the lower part of the pendulum. The lower motor is left unconnected and serves only as a bob.

to a file in the NXT controller, we have calculated the evolution of the pendulum length in time. Two periods of the modulation are shown in Fig. 2 (c) — the one is for the initial ($\approx 40^\circ$) and the other one for the final amplitude ($\approx 100^\circ$). The elongation of the modulation period is easily seen. When the motor power is set correctly, the increase of the amplitude from 10° to 100° has been routinely observed. In this case the maximum amplitude is reached after about 36 s. It is worth to note that when the power stabilization option in the *Motor Block* in the program was enabled, indeed no parametric resonance was experimentally observed, since the motor period does not follow the changes in the period of the pendulum.

On the basis of the video recording of the parametric resonance we have measured the amplitude of the pendulum versus time, as shown with crosses in Fig. 2 (d). On the

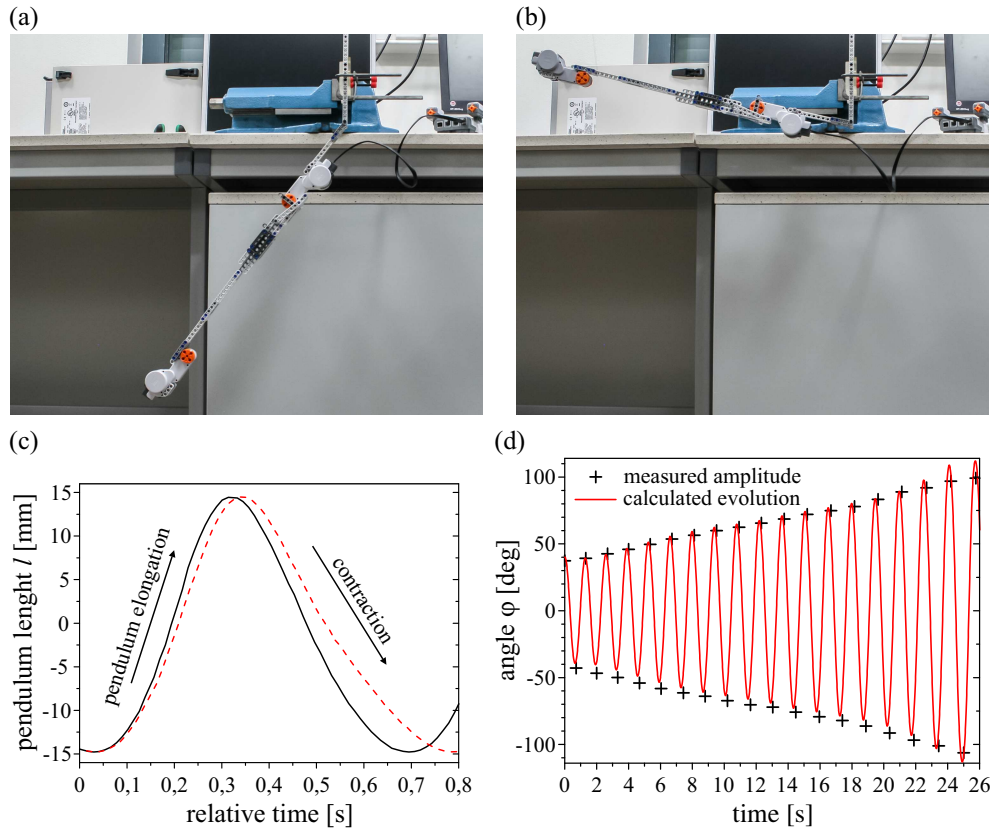


Figure 2. Initial (a) and maximum (b) amplitude of the pendulum, (c) evolution of the pendulum length for initial (solid, black line) and final (dashed, red line) swings, i.e. for relatively small (40°) and large ($\approx 100^\circ$) amplitudes. This behaviour is crucial for the efficient parametric resonance excitation — see text for details, (d) the amplitude measured on the basis of pictures taken with an amateur hybrid camera (crosses) and the numerical simulation (red line).

other hand, we have numerically solved Eq. 5 for $l_0 = 0.404$ m and $\alpha/m = 0.106$ 1/s. The latter value was found experimentally for the case of the unmodulated pendulum. In the function $f(t)$ the geometry of the motor, arm and rod from Fig. 1 (b) was taken into account. In particular, the peak-to-peak change of the pendulum reduced length was 28.6 mm and the shape of the function is seen in Fig. 2 (c). The numerical results are plotted with red line in Fig. 2 (d). To achieve a very good correspondence between measurements and calculations, a fine tuning of the initial angle of the motor had to be performed. The increase of the amplitude in the higher angles range (above 60°) deviates from an exponential one, since the period of the modulating motor does not perfectly fit half of the period of the pendulum.

The program allowing to control the motor power and measure and save the motor phase is available in the supplementary data section: *parametric_resonance.rbt*. A movie with a similar presentation of the parametric resonance is included in the supplementary data section — *parametric_resonance.avi* file.

3.2. Ultrasonic sensor

The quantification of the pendulum oscillations shown in the previous section was based on the manual analysis of the frames extracted from the recorded movie. This procedure may be simplified when using high speed cameras and a dedicated software (See Ref. [23]) or, by simply applying an ultrasonic distance sensor, included in the basic LEGO Mindstorms NXT set. The idea of the measurement is shown in Fig. 3.2 (a) and (b). The distance between the ultrasonic sensor and a screen (cardboard, mounted in such a way that it keeps vertical orientation despite pendulum inclination) is recorded and the angle of inclination is straightforwardly computed from the geometric relations. The

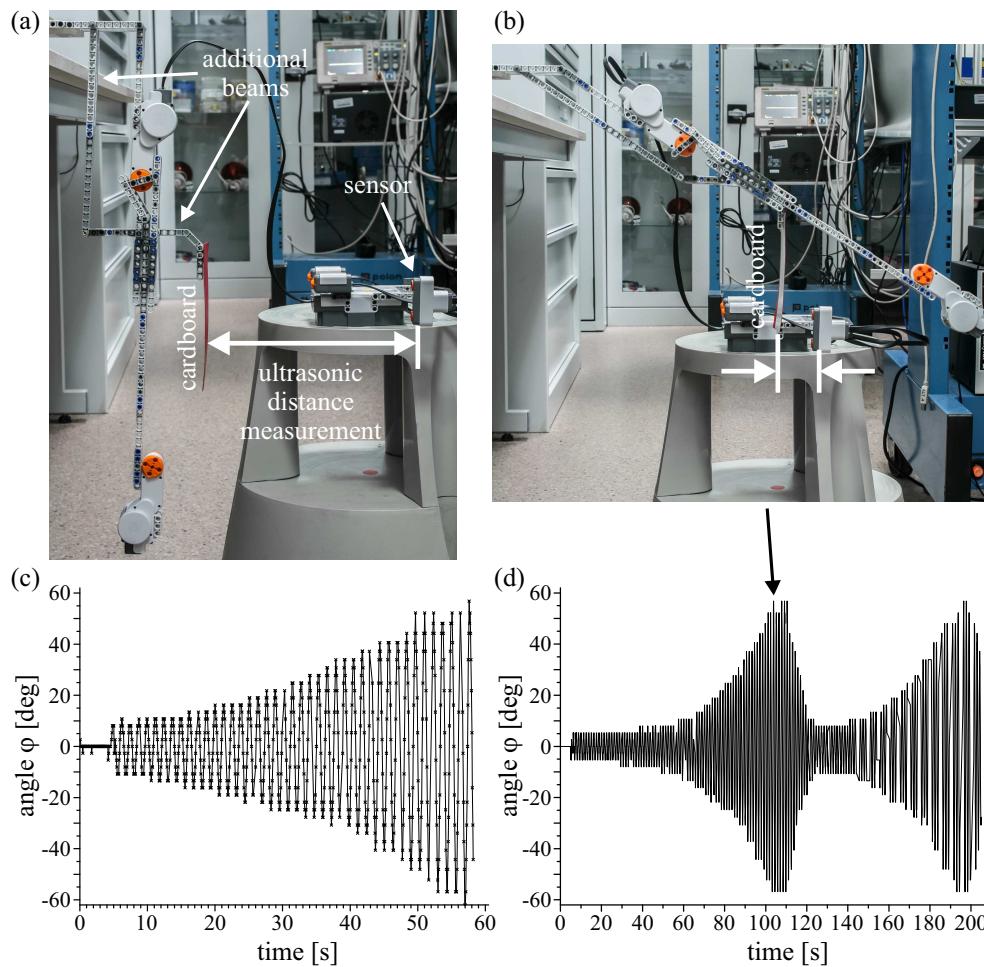


Figure 3. Pendulum with the ultrasonic sensor: (a) principle of the measurement, (b) pendulum at maximum inclination (limited by the presence of the sensor), (c) a typical evolution of the pendulum inclination. The line is added to guide an eye, (d) longer evolution, showing the revival of the parametric resonance.

resolution of the sensor readout is 1 cm, so the calculated angle resolution in the worst case (at maximum inclination) is 5° . A short movie presenting the parametric resonance in this configuration is available in the supplementary data section — see *ultrasonic.mp4* file. In Fig. 3 (c) there is shown a typical result of the measurement for the initial angle

of inclination as low as 10° . The interplay between the phase of the modulating motor, the amplitude of the oscillations and the motor power usually leads to a cyclic revival of the parametric resonance, as shown in Fig. 3 (d). Some irregularities seen in the plot after 140 s are due to limited capabilities of saving data to a file in the NXT brick. The program for this version of the pendulum is available in the *ultrasonic.rbt* file.

3.3. Absolute orientation sensor

Full and precise information about the pendulum movement may be retrieved with an inertial sensor mounted directly on the pendulum arm — see Fig. 4 (a). The sensor and its casing with batteries serve also as a bob. To avoid unwanted friction caused by a wire connecting sensor and a computer, we have implemented a wireless radio data transfer. In our case the sensor provides actual time, the values of the angle around x axis, x

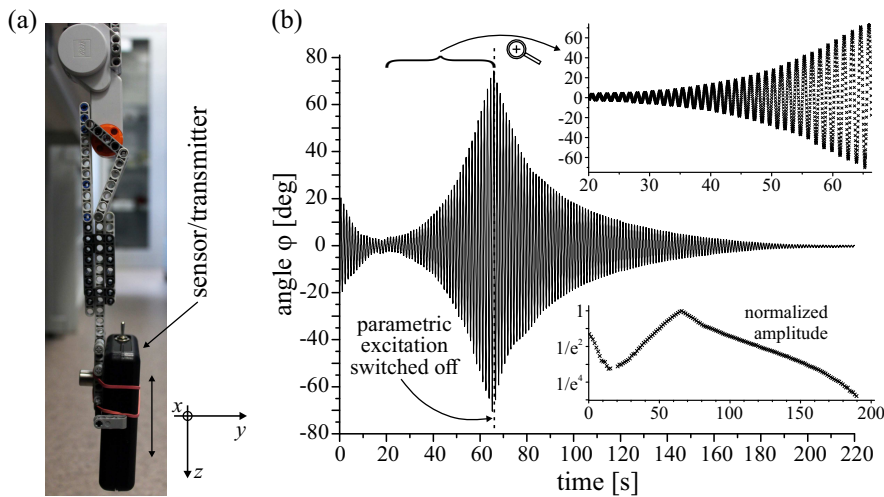


Figure 4. (a) the sensor mounted at the end of the pendulum. The sensor local coordinate system is also shown, (b) typical results for the pendulum equipped with the absolute orientation sensor. The data were collected every 20 ms. Around 65 s the excitation was switched off allowing to measure the damping constant. The upper inset shows the magnification of the most interesting part of the graph. In the lower inset the amplitude of the oscillations is shown in the semi-logarithmic scale.

component of the angular speed and y and z components of the linear acceleration. The local coordinate system of the sensor is also depicted in Fig. 4 (a). The data are transmitted every 20 ms and may be recorded to a file and displayed in real time on a computer screen — see the *imu.mp4* movie in the supplementary data section for the case of an unmodulated pendulum. More information about the wireless sensor is provided in Sec. 5.

In Fig. 4 (b) a plot of the angle versus time is shown. The initial inclination of the pendulum was 20° . At the beginning, the amplitude of the oscillations drops due to unfavorable phase relation between the motor and the pendulum inclination [20]. At about 20 s the amplitude starts growing until it reaches about 75° , as shown in

magnification in the upper inset. At 65 s the motor was stopped, thus the common damped oscillations are seen. The changes of the amplitude in the semi-logarithmic scale are shown in the lower inset. For angles below 60° , the amplitude changes are to a good approximation linear, confirming the expected exponential behaviour. An exemplary movie illustrating parametric resonance for the pendulum with the sensor is available in the *pendulum_imu.avi* file.

4. Parametric resonance with cold atoms

Originally, we have used the LEGO Mindstorms setup during the lectures on experimental techniques in atomic physics to illustrate the parametric resonance phenomenon in case of cold atoms trapped in a dipole optical trap [24]. A scheme of a dipole trap and typical experimental results are shown in Fig. 5. In our case the dipole trap is formed by two focused laser beams, red-detuned from an atomic optical resonance which intersect at their waists. The trapping mechanism rely on the interaction between the intensity gradient of the laser light (hence focused laser beam) and the group of atoms, which emerges as optical dipole force between them. The optical dipole force is conservative, so that we can introduce an optical potential which can be either attractive or repulsive depending on the detuning sign. Since we need an attractive potential (trapping), we use red-detuned light and atoms are oscillating around the point of the highest intensity. One of the most important parameters that

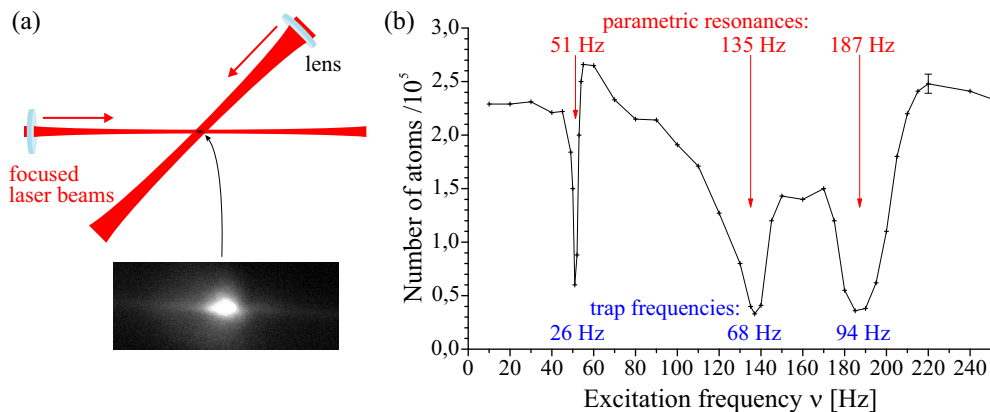


Figure 5. (a) Schematic representation of the optical trap configuration along with fluorescence image of rubidium atoms in the optical dipole trap, (b) result of the trap frequency measurement, performed during preparation of an atom laser described in Ref. [25]. The line is added to guide an eye.

characterizes the optical dipole trap is the trap frequency (to be more precisely three trap frequencies, due to the trap anisotropy). It is difficult to accurately compute the trap frequency because it depends on the potential shape and it is hard to include the laser beam shape details and imperfections in the calculations. Here, the parametric resonance is of a great help. Let the trap frequency correspond to the single frequency ω_0 in our pendulum. The excitation of the atom trap is realized by the modulation of

the intensity of the laser beam. The modulation at a doubled trap frequency leads to a strong energy redistribution in the atomic cloud and part of the atoms acquire the excess of the kinetic energy that is high enough to leave the trap. This way, when the parametric resonance condition is fulfilled, the trap population substantially decreases what is easily observed in the experiment, as shown in Fig. 5 (b). The excitation frequency, divided by 2, gives the final result — the trap frequency.

5. Technical notes

In this section we shortly present the wireless inertial sensor mentioned in Sec. 3.3. Since there are several methods of collecting and transmitting data from the inertial sensors (including WiFi and Bluetooth equipped microcontrollers and boards) and lots of tutorials and resources may be found in Internet, we focus only on the main features of the sensor. Our system is schematically shown in Fig. 5 (a) along with the pictures of the actual realizations of the sensor/transmitter and the receiver. We have used

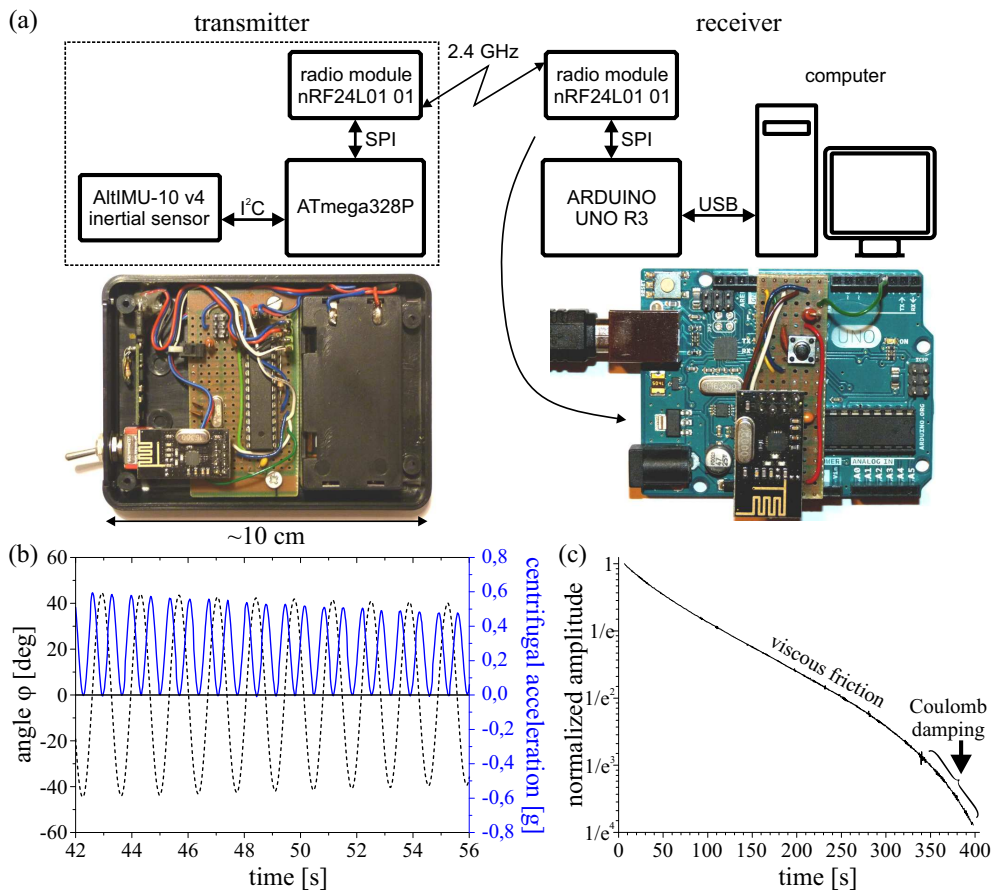


Figure 6. (a) general scheme of the wireless inertial sensor (see text for details), (b) exemplary results (angle and acceleration component) for a damped, unperturbed pendulum, (c) evolution of the normalized amplitude. The domination of various dissipative forces is easily seen.

AltIMU-10 v4 board by Pololu as an absolute orientation sensor. It consists of a MEMS

gyroscope, accelerometer, compass, and pressure sensors [26]. The board communicates with an Atmel microcontroller ATmega328P via I²C bus. The microcontroller plays two roles. The first one is to join and filter out noisy and biased data from the sensors and the second one is to send them via SPI bus to the radio transmitter. Here we have implemented a popular nRF24L01+ single chip transceiver working in the 2.4 GHz band. The data are received by a similar module and re-sent to a computer via virtual serial port with the help of the Arduino UNO R3 board. The measured values of the angle and components of the angular velocity and linear acceleration are recorded to a text file and displayed with the help of a Python script (see supplementary data section — *imu.mp4* file). The casing of the sensor is relatively large ($10 \times 7 \times 2.5 \text{ cm}^3$) but may be easily miniaturized if needed. The current consumption of the sensor/transmitter is below 10 mA only. The presented wireless sensor is a simple yet powerful and handy tool and may be easily copied since it was designed on the basis of well known and documented boards. The sensor and the Arduino board were programmed with Arduino Integrated Development Environment, basing on dedicated open-access libraries and partially modified programs, listed in the supplementary data section with additional comments — see *software.pdf* file.

We have tested the usefulness of the AltIMU-10 v4 sensor with DCM (Direction Cosine Matrix) and complementary filtering algorithm for the quantitative measurements of the (quasi)periodic motion in the following way. The sensor was attached to a rigid pendulum made of a 65 cm long steel rod, mounted on a ball bearing. The angle, angular speed and linear acceleration were recorded for damped oscillations and compared with expected calculated values, revealing a very good correspondence. Fig. 5 (b) shows part of the data — angle and centrifugal acceleration evolution. The proper shape and relative phase of both plots were achieved after introducing corrections to the original filter constants (see *software.pdf* file). In Fig. 5 (c) the fading amplitude of the oscillations is presented (the amplitude is normalized to the initial inclination of the pendulum). Different regimes of the damping (kinetic friction, linear and quadratic damping) may be seen and analyzed.

We have also tested the BNO055 Bosh absolute orientation sensor with on-board implemented data fusion and filtering algorithms. The pendulum angle measurements were unfortunately substantially influenced by the embedded auto calibration procedure, leading to the addition of an artificial variable bias (up to several degrees) to the angle values.

It is worth noting that one of the other methods of recording the data retrieved from the inertial sensors is to use modern smartphones, as described in the recent years in the literature — see e.g. [27, 28].

6. Conclusions

The parametric resonance is an ubiquitous phenomenon which occurs in many physical systems described by classical or even quantum mechanics. In this article, first the

mathematical description of the parametric resonance is briefly discussed. Next, we introduce the setup based on the LEGO Mindstorms NXT set which enables the parametric resonance observation and analysis. The basic and additional ultrasonic sensor setups are built entirely with LEGO Mindstorms components and allow to perform a quantitative analysis of the amplitude evolution, damping character and damping constants of the pendulum. We also show a wireless absolute orientation sensor, which may be used in a comprehensive analysis of driven or free pendulum movement. Finally, illustration of the parametric resonance in the conservative atomic trap for cold atoms is discussed.

Since LEGO Mindstorms sets are very popular and can often be found at physics, engineering and computer science faculties we think that our approach may be successfully employed in high schools, during science shows and even during lectures on advanced atomic physics to easily visualize parametric resonance phenomenon. Moreover, the wireless absolute orientation sensor itself may be used in the introductory student laboratories or in student projects, for example to measure the efficiency of pumping a swing with different techniques.

Acknowledgments

We are grateful to David Guéry-Odelin for fruitful discussions, Stanisław Pajka for technical assistance and Maciej Kawalec for the help with the LEGO Mindstorms set.

References

- [1] Nayfeh A H and Mook D T 1995 *Nonlinear oscillations* (Wiley)
- [2] Turner K L, Miller S A, Hartwell P G, MacDonald N C, Strogatz S H and Adams S G 1998 *Nature* **396** 149–152
- [3] Fossen T and Nijmeijer H (eds) 2012 *Parametric Resonance in Dynamical Systems* (Springer-Verlag New York)
- [4] Landau L D and Lifshitz E M 1969 *Mechanics, Vol. 1 of A Course of Theoretical Physics* 2nd ed (Pergamon Press)
- [5] Lego Mindstorms EV3 [online] [access: 2016-08-18] URL <http://www.lego.com/en-gb/mindstorms>
- [6] Kawalec T and Bartoszek-Bober D 2012 *Eur. J. Phys.* **33** 85–90
- [7] Yasin M, Böhm S, Gaggero P O and Adler A 2011 *Physiological Measurement* **32** 851865
- [8] de la Torre L, Sánchez J, Dormido S, Sánchez J P, Yuste M and Carreras C 2011 *Eur. J. Phys.* **32** 571–584
- [9] Savard T A, O’Hara K M and Thomas J E 1997 *Phys. Rev. A* **56** 1095–1098
- [10] Ju Y 2005 *Physics Education* **40** 534–536
- [11] Pinto F 1993 *The Physics Teacher* **31** 336–346
- [12] Butikov E I 2013 *International Journal of Non-Linear Mechanics* **55** 25–34
- [13] Butikov E I 2004 *Eur. J. Phys.* **25** 535–554
- [14] Case W B 1996 *American Journal of Physics* **64** 215–220
- [15] Case W B and Swanson M A 1990 *American Journal of Physics* **58** 463–467
- [16] Wirkus S, Rand R and Ruina A 1998 *The College Mathematics Journal* **29** 266–275
- [17] Roura P and González J A 2010 *Eur. J. Phys.* **31** 1195–1207

- [18] Linge S O 2012 *Computer Methods in Biomechanics and Biomedical Engineering* **15** 1103–1109
- [19] Dittrich W, Minkin L and Shapovalov A S 2013 *The Physics Teacher* **51** 163–165
- [20] Leroy V, Bacri J C, Hocquet T and Devaud M 2006 *Eur. J. Phys.* **27** 469–483
- [21] Falk L 1979 *American Journal of Physics* **47** 325–328
- [22] Goldstein H, Poole C and Safko J 2001 *Classical mechanics* 3rd ed (Addison Wesley)
- [23] PhysMo [online] [access: 2017-01-10] URL <http://physmo.sourceforge.net/>
- [24] Grimm R, Weidemüller M and Ovchinnikov Y B 2000 *Adv. At. Mol. Opt. Phys.* **42** 95–170
- [25] Couvert A, Jeppsen M, Kawalec T, Reinaudi G, Mathevet R and Guéry-Odelin D 2008 *Europhys. Lett.* **83** 50001
- [26] Altimu-10 v4 [online] [access: 2017-01-10] URL <https://www.pololu.com/product/2470>
- [27] Monteiro M, Cabeza C and Martí A C 2014 *Eur. J. Phys.* **35** 045013
- [28] Castro-Palacio J C, Velázquez-Abad L, Giménez M H and Monsoriu J A 2013 *American Journal of Physics* **81** 472–475